PLOS ONE

RESEARCH ARTICLE

Defeating a superbug: A breakthrough in vaccine design against multidrug-resistant *Pseudomonas aeruginosa* using reverse vaccinology

Sepideh Fereshteh[1☯], Fatemeh Haririzadeh Jouriani[1☯], Narjes Noori Goodarzi[2], Mahdi Torkamaneh[1], Behnoush Khasheii[3], Farzad Badmasti[1]*

1 Department of Bacteriology, Pasteur Institute of Iran, Tehran, Iran, **2** Department of Pathobiology, School of Public Health, Tehran University of Medical Sciences, Tehran, Iran, **3** Department of Pathobiology, Faculty of Veterinary Science, Bu-Ali Sina University, Hamedan, Iran

☯ These authors contributed equally to this work.
* fbadmasti2008@gmail.com

Citation: Fereshteh S, Haririzadeh Jouriani F, Noori Goodarzi N, Torkamaneh M, Khasheii B, Badmasti F (2023) Defeating a superbug: A breakthrough in vaccine design against multidrug-resistant *Pseudomonas aeruginosa* using reverse vaccinology. PLoS ONE 18(8): e0289609. https://doi.org/10.1371/journal.pone.0289609

Editor: Sheikh Arslan Sehgal, The Islamia University of Bahawalpur Pakistan, PAKISTAN

Received: October 27, 2022

Accepted: July 22, 2023

Published: August 3, 2023

Data Availability Statement: All relevant data are within the paper and its Supporting Information files.

Funding: No funding was allocated for this study.

Competing interests: The authors have declared that no competing interests exist.

Abstract

Background

Multidrug-resistant *Pseudomonas aeruginosa* has become a major cause of severe infections. Due to the lack of approved vaccines, this study has presented putative vaccine candidates against it.

Methods

P. aeruginosa 24Pae112 as a reference strain was retrieved from GenBank database. The surface-exposed, antigenic, non-allergenic, and non-homologous human proteins were selected. The conserved domains of selected proteins were evaluated, and the prevalence of proteins was assessed among 395 genomes. Next, linear and conformational B-cell epitopes, and human MHC II binding sites were determined. Finally, five conserved and highly antigenic B-cell epitopes from OMPs were implanted on the three platforms as multi-epitope vaccines, including FliC, the bacteriophage T7 tail, and the cell wall-associated transporter proteins. The immunoreactivity was investigated using molecular docking and immune simulation. Furthermore, molecular dynamics simulation was done to refine the chimeric cell-wall-associated transporter-TLR4 complex as the best interaction.

Results

Among 6494 total proteins of *P. aeruginosa* 24Pae112, 16 proteins (seven OMPs and nine secreted) were ideal according to the defined criteria. These proteins had a molecular weight of 110 kDa and were prevalent in $\geq$ 75% of *P. aeruginosa* genomes. Among the presented multi-epitope vaccines, the chimeric cell-wall-associated transporter had the strongest interaction with TLR4. Moreover, the immune simulation response revealed that the bacteriophage T7 tail chimeric protein had the strongest ability to stimulate the immune system. In

addition, molecular docking and molecular dynamic simulation indicated the proper and stable interactions between the chimeric cell-wall-associated transporter and TLR4.

Conclusion

This study proposed 16 shortlisted proteins as promising immunogenic targets. Two novel platforms (*e.g.* cell-wall-associated transporter and bacteriophage T7 tail proteins) for designing of multi-epitope vaccines (MEVs), showed the better performance compared to FliC. In our future studies, these two MEVs will receive more scrutiny to evaluate their immunoreactivity.

1. Introduction

Pseudomonas aeruginosa is a ubiquitous Gram-negative bacterium that belongs to the *Pseudomonadaceae* family and can survive in a variety of environments, including soil and water. Indeed, it can be easily found in almost any human- or animal-influenced habitat [1]. Studies have shown that in healthcare settings, this bacterium causes fatal nosocomial infections such as pneumonia, urinary tract infections, wound infections, and septicemia, especially in immunocompromised individuals [2, 3]. In addition, *P. aeruginosa* is responsible for more than 5% of infectious exacerbations in patients with chronic obstructive pulmonary disease (COPD) and has been associated with increased mortality in these patients [4]. In 2017, carbapenem-resistant *P. aeruginosa* was recognized as one of the most life-threatening bacteria and listed by the World Health Organization (WHO) as a priority pathogen for the research and development of new ways to overcome it [5].

The overuse of antibiotics during treatment accelerates the development of multidrug-resistant *P. aeruginosa* strains, leading to the ineffectiveness of antibiotic therapy against this microorganism [6]. Therefore, there is an urgent need to discover new strategies for the prevention of severe *P. aeruginosa* infections. To date, different approaches, such as secondary metabolites, nanomaterials, and vaccine development, have been suggested to find a suitable alternative to the currently used antibiotics against this pathogen. However, because of ongoing problems such as growing antibiotic resistance and population aging, vaccination could be more desirable and cost-effective [7, 8].

Currently, numerous vaccine development methods are being tested against this superbug. For example, whole-cell vaccines [9], killed and attenuated live vaccines [10, 11], outer membrane vesicles (OMVs) [12], outer membrane complexes (OMCs) [13], flagella [14], pilins [7], and glycol-conjugate vaccines [15] have been proposed as promising vaccination approaches against *P. aeruginosa*. Although many of these approaches have been tested experimentally in preclinical trials, few of them have reached the clinical phase, and none of them has been approved for marketing [7]. Therefore, in the absence of an effective vaccine, efforts are continuing.

Present immunization strategies mainly concentrate on outer membrane proteins (OMPs) as desirable subunit vaccines since there is no risk of the pathogen reverting to its virulent form and there are few adverse effects compared to live attenuated, or killed whole-cell vaccines [7]. Moreover, on the surface of bacterial cells, OMPs play a key role in bacterial physiology and pathogenesis; therefore, they are considered prime targets for vaccine development [16]. In this regard, reverse vaccinology (RV) allows researchers to use the whole bacterial genome sequence to find immunogenic and surface-exposed proteins and study them from

different aspects such as antigenicity, allergenicity, and similarity to the human proteome [17, 18]. As a result, a new generation of vaccines can be developed based on antigens that were previously not detected or even ignored. For example, RV has been successfully used to produce the 4CMenB vaccine (Bexsero, GSK) as the first approved vaccine against *Neisseria meningitidis* serogroup B (MenB), which is currently licensed in several countries [19, 20].

Taking into account the aforementioned, the present study aimed to investigate the whole genome sequence of *P. aeruginosa* 24Pae112 to introduce novel and putative vaccine candidates. Also the design of new multi-epitope vaccines against this bacterium can be considered as promising subunit vaccines. The obtained results from this study provide new insights into vaccine development not only against *P. aeruginosa* but also against other Gram-negative bacteria.

2. Materials and methods

2.1. Consecutive analyses

2.1.1 Genomes sequence retrieval. In the first step, 395 completed genomes of *P. aeruginosa* were retrieved from the GenBank database (https://www.ncbi.nlm.nih.gov/genbank/) and extracted to the proteome using CLC Genomics Workbench Software (Qiagen, Hilden, Germany) [21] to perform core/pan-genome analysis using BPGA (Bacterial Pan Genome Analysis Tool) software [22]. After genome evaluation, *P. aeruginosa* 24Pae112 (accession number: NZ_CP053028.1), which belongs to ST235, was selected as a reference strain. *P. aeruginosa* ST235 is spread around the world, possibly due to selective pressure from fluoroquinolones, and became easily resistant to aminoglycosides, beta-lactams, and carbapenems through mutation and acquisition of resistance elements [23].

2.1.2 Prediction of subcellular localization. All proteins were uploaded to the PSORTb database (https://www.psort.org/psortb/) to predict their subcellular localization [24]. In this step, extracellular, secreted, and surface-exposed proteins were considered. The results were confirmed using the TMHMM Server v. 2.0 web tool (https://services.healthtech.dtu.dk/service.php?TMHMM-2.0) to identify surface-exposed regions [25].

2.1.3 Antigenicity and allergenicity determination. The antigenicity of putative immunogenic proteins was predicted using the VaxiJen online tool (http://www.ddgpharmfac.net/vaxijen/VaxiJen/VaxiJen.html) with a cut-off value of $\geq$ 0.4 and ANTIGENpro (https://scratch.proteomics.ics.uci.edu/) [26, 27]. On the other hand, the allergenicity of the putative immunogenic proteins was predicted using AlgPred 2.0 (http://crdd.osdd.net/raghava/algpred/) with a cut-off value of $\geq$ 0.3 and AllergenFP (https://www.ddg-pharmfac.net/AllergenFP/) [28, 29].

2.1.4 Homology analysis of immunogenic targets against the human proteome. All selected proteins were analyzed to determine their sequence similarity to the human proteome (*Humo sapiens*, Taxid: 9606) using the PSI-BLAST tool in the BLASTp database (https://blast.ncbi.nlm.nih.gov/Blast.cgi?SIDE=protein) [30]. Proteins showing any similarity to the proteome of the host were excluded from the study.

2.1.5 Functional class determination and molecular weight estimation. First, the functional class of the selected proteins was determined using the VICMpred database (https://webs.iiitd.edu.in/raghava/vicmpred/submission.html) [31]. Then, the number of amino acids and molecular weights were determined using the Expasy ProtParam server (https://web.expasy.org/protparam/) [32].

2.1.6 Protein domain search. Conserved Domain Database, CDD (https://www.ncbi.nlm.nih.gov/Structure/cdd/cdd.shtml) and EggNOG (http://eggnog5.embl.de/#/app/home) were used to find the protein domains. CDD is a part of the NCBI's Entrez query and provides

annotation of protein sequences with the position of the conserved domain [33]. EggNOG is an annotated orthology resource according to 5090 organisms and 2502 viruses [34].

2.1.7 Prevalence of putative immunogenic targets among *P. aeruginosa* genomes dataset. Whole genome sequences of 395 *P. aeruginosa* strains were checked using BPGA software, and the prevalence matrix as software output was used to determine the prevalence of each protein [22]. In this step, the cut-off value of $\geq$ 75% was considered.

2.2. Immunoinformatics analyses

2.2.1 Determination of linear B-cell epitopes and human MHC II binding sites. The BepiPred-2.0 tool (https://services.healthtech.dtu.dk/service.php?BepiPred-2.0) was used to identify linear B-cell epitopes of all previously selected proteins with a threshold of $\geq$ 0.6 [35]. The B-cell epitope ratio (number of amino acids of all epitopes divided by the total amino acids of each protein) was calculated for each protein, and proteins with a ratio above the average were selected. In the next step, TepiTool (http://tools.iedb.org/tepitool/), an IEDB resource, was used to predict human MHC II binding sites with a cut-off of the top 5% of peptides [36]. The ratios of MHC II binding sites (the number of MHC II binding sites divided by the total amino acids of each protein) were calculated.

2.2.2 Quartile scoring method. The selected proteins were analyzed by the quartile scoring method using three different indicators, including antigenicity, linear B-cell epitope, and MHC II binding site ratios. The sum of all scores for each protein was considered the final score [21].

2.2.3 Tertiary structure prediction and characterization of conformational B-cell epitopes. The tertiary structure (3D) of the putative immunogenic proteins was predicted using the Robetta tool (https://robetta.bakerlab.org/) [37]. The quality of the 3D model was checked using the ProSA web server (https://prosa.services.came.sbg.ac.at/prosa.ph) [38]. This server shows the potential errors in the 3D model. The energetically refused and permitted regions were predicted using Ramachandran plots at the Zlab Ramachandran Plot Server (https://zlab.umassmed.edu/bu/rama/index.pl) [39]. ElliPro (http://tools.iedb.org/ellipro/) was used to identify the conformational B-cell epitopes with a threshold of $\geq$ 0.8 [40]. The predicted conformational B-cell epitopes were displayed on the surface of each protein in different colors using the Jmol software [41].

2.2.4 Protein-protein interaction based on the STRING database. In this part, we used the STRING database (https://string-db.org/) to investigate the interactions of two Hypothetical proteins with other proteins of *P. aeruginosa* to estimate their function. In molecular biology, STRING is a biological database and web resource for known and predicted protein-protein interactions [42].

2.3. Construction of multi-epitope vaccines

2.3.1 Selecting antigenic and conserved linear B-cell epitopes. Linear B-cell epitopes, located on the extracellular loops of seven OMPs selected from previous steps, were predicted using the BepiPred database with a cut-off value of $\geq$ 0.6. Additionally, the conservation of linear B-cell epitopes was determined using the ConSurf web tool (https://consurf.tau.ac.il/consurf_index.php) [43].

2.3.2 Implantation of conserved linear B-cell epitopes on platforms. Three multi-epitope-based vaccines were generated using three different platforms obtained from *P. aeruginosa* strain 24Pae112, including FliC (WP_124119965.1), bacteriophage T7 tail protein (WP_166796845.1), and cell-wall-associated transporter (WP_024947839.1). The tertiary (3D) structures of these chimeras were modeled using the Robetta web tool. The 3D structures were

validated by the ProSA web server (https://prosa.services.came.sbg.ac.at/prosa.php) and Ramachandran Plot (https://zlab.umassmed.edu/bu/rama/).

2.3.3 Molecular dockings and immune simulations. Molecular dockings and the binding affinities of three multi-epitope vaccines to human TLR1 (PDB: 2Z7X), TLR2 (PDB: 2Z7X), and TLR4 (PDB: 3FXI) were assessed with pyDockWEB (https://life.bsc.es/pid/pydockweb/default/index). In addition, C-ImmSim (https://kraken.iac.rm.cnr.it/C-IMMSIM/index.php) was used to predict the simulation of the immunoreactivity of multi-epitope vaccines [21]. Finally, PDBsum (http://www.ebi.ac.uk/thornton-srv/databases/pdbsum/) was used to reveal the paired residues of the chimeric cell-wall-associated transporter and TLR4 [44].

2.3.4 Molecular dynamics simulation of the selected vaccine in complex with the immune receptor. Molecular dynamics (MD) simulation was done to refine the chimeric cell-wall-associated transporter-TLR4 complex using the GROMACS version 2018 simulation package. The structure was centered in a dodecahedron box and filled with water using the TIP3 water model. To neutralize the system, some molecules of water were randomly replaced by Cl^- or Na^+. After neutralization, the energy minimization (5000 steps) was done using the steepest descent algorithm. Equilibrating the system was performed under 100 ps NVT at a temperature of 298 K, followed by 100 ps NPT ensembles at a pressure of 1 bar. Electrostatic interactions were calculated by PME, and the LINCS procedure was applied to constrain all bonds connecting hydrogen atoms. The final MD simulation was run for 100 ns with no restraint [45, 46].

3. Results

3.1. Core/pan-genome analysis and subcellular localization prediction

The core/pan-genome ratio and B-parameter (0.24) obtained from BPGA analysis on 395 completed genomes of *P. aeruginosa* revealed that this bacterium has a wide genome. These results indicated the plasticity of the *P. aeruginosa* genome due to many insertion and deletion events. Therefore, using the core proteome was not proper, and we used the whole genome of *P. aeruginosa* 24Pae112 instead (Fig 1A). The KEGG (Kyoto Encyclopedia of Genes and Genomes) distribution plot revealed that the majority of core, accessory, and unique genes were involved in the metabolism of this pathogen (Fig 1B). *P. aeruginosa* strain 24Pae112 showed that the genome has a total of 6494 proteins. Among them, a total of 241 surface-exposed proteins consisting of 167 OMPs and 74 extracellular proteins were identified, and others were excluded. The workflow for identifying new immunogenic targets and designing multi-epitope vaccines against *P. aeruginosa* 24Pae112 has been presented in Fig 2.

3.2. Consecutive analysis revealed desirable proteins

Back-to-back analysis of selected proteins from the previous step, revealed that out of 241 proteins, 92 were antigenic, non-allergenic, and non-homologous to human proteins. Therefore, these proteins were selected for further analysis.

3.3. Subtraction of the proteins based on molecular weight and prevalence

According to the defined criteria, 72 proteins with a molecular weight < 110 kDa and a prevalence $\geq 75\%$ among *P. aeruginosa* genomes were selected. These proteins were involved in different functional classes, including virulence (22 proteins), cellular processes (35 proteins), metabolism (13 proteins), and information and storage (two proteins). See the S1 Table.

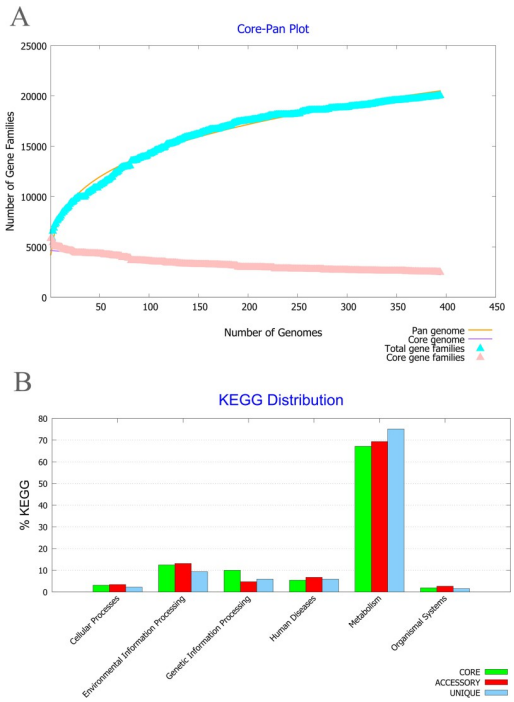

Fig 1. Core-proteome analysis using the BPGA database. A) The core/pan plot of 395 *P. aeruginosa* strains showed a total of 2547 core proteins. **B)** The KEGG distribution of core, accessory, and unique genes of *P. aeruginosa* strains represented that the majority of all three categories are involved in the metabolism of this pathogen.

https://doi.org/10.1371/journal.pone.0289609.g001

3.4. Quartile scoring assessment to select shortlisted proteins

All selected proteins were assessed using the quartile scoring method. Finally, a total of 16 proteins (seven OMPs and nine secreted) with a contractual score ≥ 7 were considered shortlisted proteins and valuable for further investigations. The accession numbers for these proteins are as follows: Hypothetical proteins (WP_132548232.1 and WP_166796845.1), Type I fimbrial protein (WP_034004502.1), Type II secretion system secretin GspD (WP_061193930.1), Hcp family type VI secretion system effector (WP_110726056.1), TonB-dependent receptors (WP_023101627.1 and WP_125941151.1), Glycosyl hydrolase family 18 protein (WP_034004678.1), Type IVa pilus secretin PilQ (WP_132905315.1), Transporter (WP_024947839.1), OprD family porin (WP_003090815.1, WP_217385706.1, WP_019681707.1, and WP_243702750.1), Type III secretion system needle length determinant (WP_210733189.1), and Peptidoglycan-associated lipoprotein Pal (WP_058148283.1). See Fig 3.

3.5. Illustration of conformational B-cell epitopes and protein classification based on conserved domains

A quality assessment of the tertiary structures of proteins showed that the predicted structures are of acceptable quality. See S1 Fig. The 3D structure prediction of 16 shortlisted proteins and their conformational B-cell epitopes located on the surface of each protein is illustrated in Fig 4. Additionally, information about the predicted B-cell epitopes of seven OMPs is presented in Table 1. In the next step, proteins were classified into six different groups according to their conserved domains, including (I) Secretion system-associated proteins and transporters; (II) OprD family outer membrane proteins; (III) Fimbrial proteins; (IV) TonB-dependent

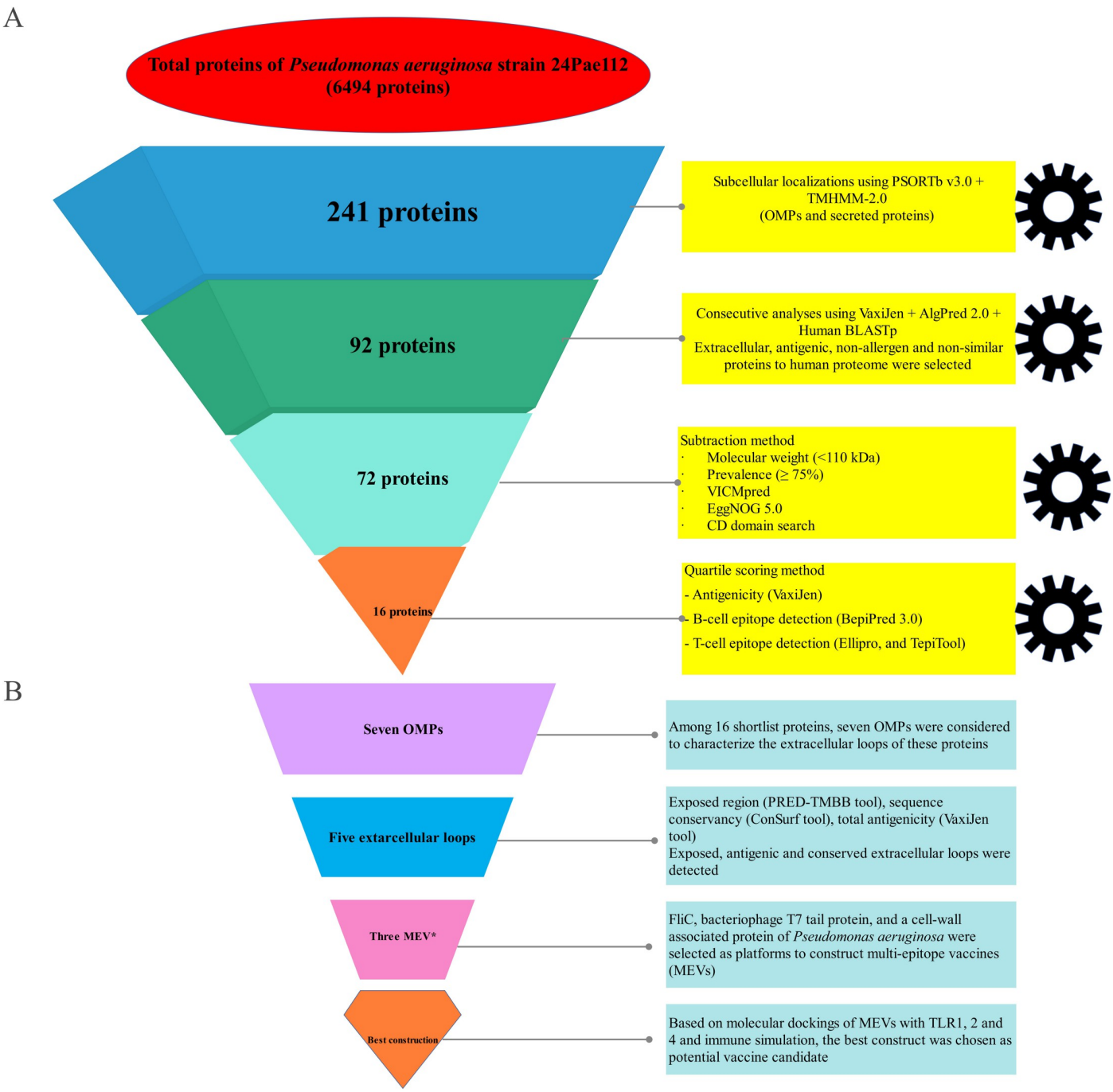

Fig 2. Schematic representation of the selection and validation of new putative immunogenic targets and multi-epitope-based vaccines against *P. aeruginosa* strain 24Pae112 using reverse vaccinology approaches and bioinformatics tools. All criteria and thresholds are shown in the flowchart. OMPs, outer membrane proteins; MEVs, multi-epitope vaccines.

https://doi.org/10.1371/journal.pone.0289609.g002

receptors; (V) Peptidoglycan-associated proteins; and (VI) Unknown-function proteins (Hypothetical proteins).

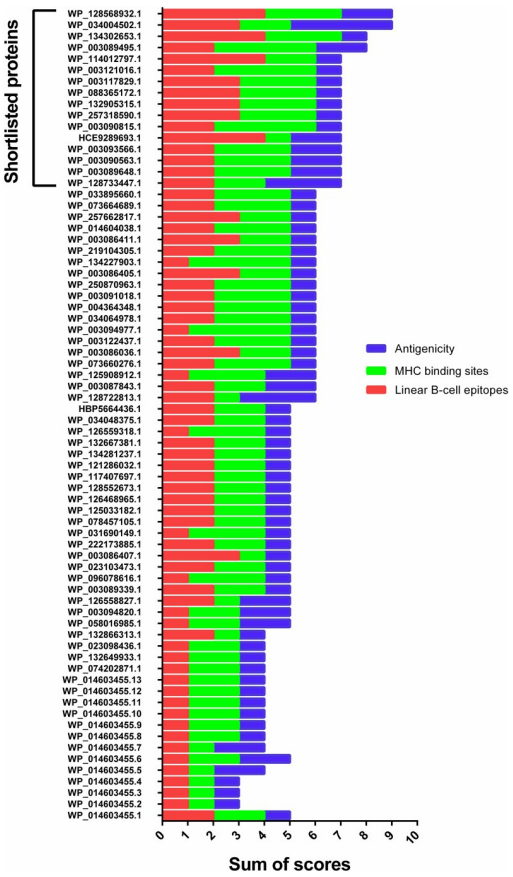

Fig 3. Comparative analysis of putative immunogenic targets against *P. aeruginosa* strain 24Pae112 based on the quartile scoring method. Sixteen proteins with a score ≥ 7 were selected, including Hypothetical proteins (WP_132548232.1 and WP_166796845.1), Type I fimbrial protein (WP_034004502.1), Type II secretion system secretin GspD (WP_061193930.1), Hcp family type VI secretion system effector (WP_110726056.1), TonB-dependent receptors (WP_023101627.1 and WP_125941151.1), Glycosyl hydrolase family 18 protein (WP_034004678.1), Type 4a pilus secretin PilQ (WP_132905315.1), Transporter (WP_024947839.1), OprD family porin (WP_003090815.1, WP_217385706.1, WP_019681707.1, and WP_243702750.1), Type III secretion system needle length determinant (WP_210733189.1), and Peptidoglycan-associated lipoprotein Pal (WP_058148283.1).

https://doi.org/10.1371/journal.pone.0289609.g003

3.6. Protein-protein interaction networks

According to the obtained results from the STRING database, the Hypothetical protein WP_132548232.1 had co-occurrence and co-expression with peptidase C39 domain-containing protein (PA1953) and co-occurrence with ABM domain-containing protein (PA0271). On the other hand, the Hypothetical protein WP_166796845.1 is neighboring the UvrD/REP helicase N-terminal domain protein (DR97_1795). The full results of protein-protein interaction networks are presented in Fig 5.

3.7. Designing multiple-epitope-based vaccines

Five conserved and highly antigenic B-cell epitopes, including PEEIGGKSSNN, YNVSKASSSGG, QADANGYYPAQKDYYGCEKGVDGAC (obtained from TonB-dependent receptor), GSTSQITEKSVTGD (extracted from Transporter), and YTAPG NTRGNS (obtained from OprD family porin), with rigid (EAAAK) and flexible (GPGPG) linkers, were assessed through different arrangements, and the most antigenic arrangement was selected to generate the chimeric

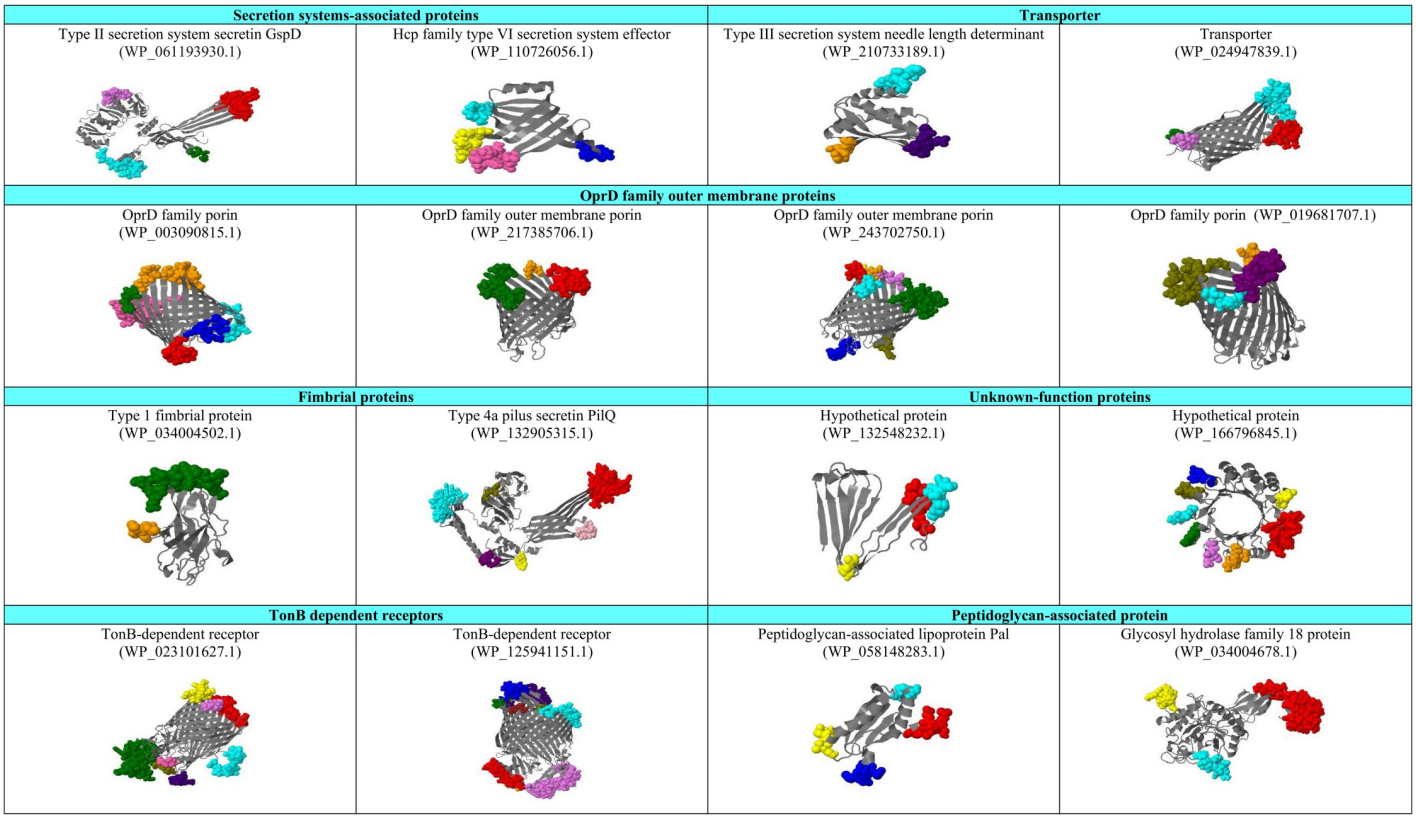

Fig 4. Surface-exposed conformational B-cell epitopes of putative immunogenic targets against *P. aeruginosa* strain 24Pae112 are illustrated in different colors. The tertiary structures of the proteins were predicted by the Robetta web tool, and the surface-exposed conformational B-cell epitopes were characterized by the 3D structure of proteins using Jmol software.

https://doi.org/10.1371/journal.pone.0289609.g004

FliC protein. To generate chimeric proteins from the bacteriophage T7 tail (WP_166796845.1) and the cell-wall-associated transporter (WP_024947839.1), the mentioned epitopes were located in the disordered regions of these platforms. The detailed data are provided in the S2 Table. The 3D structure of the multi-epitope proteins is demonstrated in Fig 6.

3.8. Molecular docking and *in silico* immunization

The pyDockWEB results demonstrated that the chimeric cell-wall-associated transporter as a multi-epitope vaccine had the strongest interactions with TLR1 (-67.516 kcal/mol), TLR2 (-52.280 kcal/mol) and TLR4 (-69.791 kcal/mol). The full results of this step are presented in Table 2. In addition, the C-ImmSim data revealed that FliC and bacteriophage T7 tail chimeric proteins induced higher levels of immunoglobulins (*e.g.* IgM and IgG1), Th1 cell population, and cytokines (*e.g.* IFN-γ and IL-2) in comparison to the cell-wall-associated transporter chimeric protein. See Fig 6. In addition, the details of interactions between cell-wall-associated transporter and TLR4 are presented in Fig 7.

3.9. Molecular dynamics simulation of the chimeric cell-wall associated transporter in complex with the TLR4

The global structural stability of the cell-wall associated transporter-TLR4 complex was evaluated using a Root Mean Square Deviation (RMSD) plot. This plot shows how much the protein conformation has changed during MD simulation from the initial structure. The RMSD of

Table 1. The sequence of linear and conformational B-cell epitopes of seven selected outer membrane proteins from *P. aeruginosa* strain 24Pae112.

No.	Protein name	Length (aa)	Linear B-cell epitopes (cut off ≥ 0.6)	Start	End	Number of epitopes	Epitope/ amino acids ratio	Conformational B-cell epitopes	Score (cut off ≥ 0.8)	Color
1	WP_023101627.1 (TonB-dependent receptor)	964	PRMSGEAP	123	130	8	0.008	R596, D597, F600, I601, T602, V603, S604, R605, P606, G607, Y608, Y609, G610, S611, M612, M613, W614, F615, P616, D617, Q618, N619, G620, Q621, Y622, T623, D624, A625, T626, D627, P628, R629, L630, N631, N632, G633, I634, V635, T636, N637, N638, T639, N640, N641, P642, F643, E644, G645, I646, P647, F648, D649, E650, F651, G652, P653, A654, N655, V656, T657, V658, H659, P660, S661, R662, V663, T664, N665, V666, V667, R834, Q836, R837, T838, E839, N840, T841, N843	0.912	Green
			QKETYT	147	152			F508, E509, T510, D511, F512, G513, D514, F515, F563, P565, V566, E567, R568, L569, L571, F691, E692, L693, A694, P695, D696, T697	0.89	Yellow
			RNG	189	191			Q291, S294, A295, S296, S297, K298, T299, E300, N301, L302, S303, S304, V305, P306, H307, D308, D309, R310, G311, S312, F314, Q317	0.882	Cyan
			LV	269	270			R361, E365, S367, S368	0.87	Hot pink
			NGVAPQHRSASSKTENL	286	302			N329, E330, H331, L332, R396, I397, A398, D399, E400, H401, Y449, L450, P451, E452, N453, N454, P455, L456, V457	0.87	Red
			GSQAKSGSA	315	323			Y362, G363, R364, G426	0.827	Olive
			YRN	327	329			S746, L747, L748, A749, D750, G751, D752	0.825	Violet
			NQGNYFSGKKGQDRYRVYNRYGRE ESSVAKVYNAGEEVLNSSSE	342	385			P479, R480, S481, Q482, A483, Y484, R485, S486	0.812	Indigo
			RTGEI	413	417					
			PSDIFRFGTAGIYQYPLS	419	436					
			YLPENN	449	454					
			EAKSDMLTSVLAPR SQAYRSDRNWTRQD	467	494					
			EDIQPQKSVVTTLHDINANRTLRDA	526	550					
			NSKDNGISASPRREDRDMRFITVSRPGYYG SMMWFPDQNGQYTDATDP RLNNGIVTNNTNNPFEGI	581	646					
			FDEFGPANVTVHPSRVTNVVTGYNYSKKGSSRGG	648	681					
			LFETSQGTLQVE	712	723					
			DPGQM	774	778					
			TCDAAFAARLRAGANRYQRTENTPNC	819	844					
			GSYTNTQNP	851	859					
			ADKPWQVGATTPQ	893	905					
			PLAQSF	943	948					

(*Continued*)

Table 1. (Continued)

No.	Protein name	Length (aa)	Linear B-cell epitopes (cut off ≥ 0.6)	Start	End	Number of epitopes	Epitope/ amino acids ratio	Conformational B-cell epitopes	Score (cut off ≥ 0.8)	Color
2	WP_125941151.1 (TonB-dependent receptor)	953	AAKVQSLAAK	90	99	9	0.009	N774, A775, G776, D777, A778, S779, V780, D781, P782, N783, R784	0.918	Orange
			RAQQEG	116	121			D675, Y677, G678, C679, E680, K681, G682, V683, D684, C687, A750, A751, C752, R753, S754, G755, G756, L757, D758, P759, D760, S761, A762, C764, R765, L768	0.915	Red Blue
			GEDYGNTWQP	157	166					
			TAYGGSVNFT	195	204			V41, R42, G43, R44, G65, S66, G67, L68, Q69, A81, A82, P83, L84, R85, A86, A87, V88, P89, A90, A91, K92, V93, Q94, S95	0.895	Cyan
			QRQPVWANQRGFMDSYPD GNNVGYRLNPQSGRYLGD	288	323			D246, R721, W811, G812, A813, G814, D815, Y816, G817, Y865, A866, Q867, F868, Y901, L903, N904, E905, R906, A907, V909, F947, Y949, F951, G952, G953	0.881	Violet Indigo
			SCAGLGGLFGGNVAPVPGARGG YRCMTDQYYNNYWTLQT	325	363					
			QNNTRGPSF	396	404			R312, L313, N314, P315, Q316, S317, G318, R319, Y320, L321, G322, D323, A324, S325, C326, A327, G328, L329, G330, G331, L332, F333, G334, G335, N336, V337, A338, P339, P341, G342, A343, R344, G345, G346, Y347, I410, N411, A412, S413, S414, G415, D416, E428, D486, L489, G490, R491, K492, L493, G494, E495, R496, G498, P500, V501, Y502, D503, P504, D505, P506, A507, R508, L509, G510, R511, P512, L513, S514, E515, E516, E517, R519, R522	0.868	Olive brown Orange Red Blue Cyan
			PEEIGGKSSNN	426	436					
			DRVANT	452	457					
			YLGRKLGERDGYPVYDP	488	504					
			PARLGRPLSEEEWRSLRRNVTQ	506	527					
			IRPDSQYNDG	567	577					
			YNVSKASSSGG	579	589					
			FSGR	621	624			E8, A9, L10, T11, F12, D13, V14, A15, A16, G17, P18, Q45, A46, P47, A48, V49, R50, G51, P52, L53, S54, Q57, E60, Q61, R64, V454, A455, N456, T457	0.854	Violet Indigo
			QADANGYYPAQKDYYGCEKGVDGAC	663	687					
			KLLRDEAACRSGGLDPDSAQC	744	764			A274, T275, G276, D277, F278	0.851	Olive
			LARVERNAGDASVDPNRLN	768	786			P639, L640, T641, S642	0.822	Brown
			YQQSDDYPSENQRDSLDS	833	850			S39, D546, L547, P548, A549	0.817	Green
			VTNAAG	880	885					
			EDDSDGWPY	922	930					
3	WP_024947839.1 (transporter)	397	RQVEAQPQAPQPQRLVKSIQPPAQAR NDANAVAGTYGASLKDD	25	77	4	0.01	L116, L118, N119, G120, F121, L129, G130, N131, I132, G133, A174, G175, A176, G177, G178, S179, T180, S181, Q182, I183, T184, Q236, V237, P238, G239, N240, N241, N242	0.901	Cyan Green Violet
			GSTSQITEKSVTGD	178	191					
			PYGIKLKQVPGNNNLNVP	229	246					
			ESFDDINPQQGVKTG	285	299			V268, D269, P270	0.869	Red
			SKVKQDGQSWQTVSG	336	350			E208, S209, E210, S211, T212, P213	0.851	Cyan
								E284, D288, I290, N291, Q293, Q294, G295, V296, K297, T298, G299, K301, K339, Q340, D341, G342, Q343, S344, W345	0.831	Green

(*Continued*)

Table 1. (Continued)

No.	Protein name	Length (aa)	Linear B-cell epitopes (cut off ≥ 0.6)	Start	End	Number of epitopes	Epitope/ amino acids ratio	Conformational B-cell epitopes	Score (cut off ≥ 0.8)	Color
4	WP_003090815.1 (OprD family porin)	405	GTED	31	34	6	0.014	I212, P213, L214, Q215, A216, D217, Q218, I257, D258, A259, H260, F319, A320, K321, Y322, G323, V324, P325, G326, V360, Q361, S362, G363, P364, A365, K366, L368	0.872	Orange
			GKGRSGA	72	78			N1, Q3, E4, A5, A6, K7, G8, F9, V10, E11, D12, S13, S48, G49, F50, T51, Q52, G53, T54, I55, G56, I57, I107, S108, N109, E145, I146, E147, G148, V404, F405	0.868	Hotpink
			KQGDSGS	85	91			D232, S233, D234, A236, D237, Q238, N239, N241, G242, N243, R244, D272	0.849	Red
			RKSAEGRDS	161	169			F184, T185, D186, H187	0.832	Green
			DFADQNFNGN	234	243			K340, T341, A342, E343, T344, S345, N346, S380, A381, D382, D385	0.811	Blue
			TAET	341	344			L69, D70, G71, G72, K73, Q86, G87, D88, S89, G90, S91	0.81	Cyan
			DARDSYFS	382	389					
5	WP_217385706.1 (OprD family outer membrane porin)	400	DGSSANPQGASK	23	34	3	0.007	A1, F2, L3, E4, D5, G6, S48, G49, Y50, T51, E52, G53, A54, L55, G56, F57, M104, F106, S107, Q108, E144, I145, A146, G147	0.898	Red
			ADSN	74	77			R224, Q225, L226, G227, A228, G229, K230, A263, Q264, G265, G266, H267, F315, L317, R318, S319, V320, G321, V322, P323, G324, V358, Q359, S360, G361, R362, F363, K364, D365	0.883	Green Red Green
			HDPRR	86	90					
			ARDSSDAQDIRLHCKNKRYACD	160	181					
			AGAARAG	243	249					
			LAN	339	341			V196, N197, D198, G199	0.839	Orange
			ERSA	380	383					
6	WP_243702750.1 (OprD family outer membrane porin)	411	ADAGRG	29	34	8	0.019	L307, A308, P309, F310, G311, L312, P313, G314	0.907	Red
			GHA	75	77			T2, E3, E4, A5, K6, A7, P8, D9, Y10, L11, Y51, T52, P53, G54, R55, V56, G57, F58, R104, L105, G106, E107, D143, L144, D145, R146, G409, S410, L411	0.905	Green
			SGDNA	87	91			V254, G255, A256, Q257	0.894	Yellow
			EQASSSGHGDFDGYGAS	159	175			A190, S191, D192, N193, R218	0.879	Violet
			QGRSRAGA	233	240			A219, A220, F221, Y252	0.87	Orange
			GSHAPAGGAYNPLGADGRYRPLQGSG	329	354			A334, N339, P340, L341, G342, A343, D344, G345, R346, Y347	0.865	Blue
			AQAG	390	393			F368, A369, S370, G371, P372, L373, K374, L376	0.837	Cyan
								N205, Q233, G234, R235, S236	0.819	Olive
7	WP_019681707.1 (OprD family porin)	447	TPSRRD	50	55	4	0.008	R247, L248, S249, S250, Q251, L252, T253, L254, G287, G288, G289, Q290, L343, A344, F345, L346, A347, A348, P349, D350, W351	0.914	Violet
			GGSGG	94	98					
			GR	108	109			V24, P25, P26, G27, F28, V29, E30, G31, S32, S69, G70, Y71, T72, D73, T74, P75, I76, G77, V78, L123, R124, G125, L126, D127, Y162, H163, F164, L446, L447	0.865	Green
			LRNQSGHS	179	186					
			GNGTKGGIAADR	193	204					
			DQGRSQLG	265	272			A218, P219, G220, G221, S222, Q244, W246	0.839	Cyan
			TRVDPDSAG	365	373			F398, P399, A400, G401, P402, A403, K404, G405, L406	0.807	Orange
			YTAPGNTRGNS	421	431					

https://doi.org/10.1371/journal.pone.0289609.t001

TLR4 and cell-wall-associated transporter was in the range of 0.2 to 0.27 and 0.2 to 0.3, respectively. Both proteins reach stability at time 10 and remain stable after that (Fig 8A). The Root Mean Square Fluctuation (RMSF) indicates the fluctuation of protein residues over time from a reference position during simulation. According to the RMSF plot, no unusual fluctuation was observed in protein structures (Fig 8B). The compactness of the cell-wall-associated transporter-TLR4 complex was evaluated using the Radius of gyration (Rg) plot. The Rg of TLR4 was in the range of 3.19 to 3.24. While the Rg of cell-wall-associated transporter was in the range of 2.25 to 2.2. According to the result, the structures of both proteins were stable (Fig 8C). Furthermore, the Solvent Accessible Surface Area (SASA) for both proteins was calculated during the simulation. SASA indicates the accessible surface of the protein solvent or a part of a protein that is exposed to the solvent. The SASA of cell-wall-associated transporter was in the range of 168 to 18 nm^2. While the SASA of TLR4 was in the range of 270 to 277 nm^2 (Fig 8D).

4. Discussion

Nowadays, one of the most important challenges for physicians is the effective treatment of infections caused by Gram-negative pathogens due to the increasing antibiotic resistance in healthcare. Meanwhile, *P. aeruginosa* occupies a leading role among infections caused by Gram-negative rods, particularly in critically ill and immunocompromised patients. Due to antimicrobial resistance, there are severely restricted treatment options for *P. aeruginosa* infection, which has become a critical and fatal problem [47, 48]. To date, many studies have been conducted in pre-clinical and clinical trial stages to introduce an effective vaccine against this bacterium. Despite all efforts, there are still no *P. aeruginosa* FDA-approved vaccines for human administration, and recent promising candidates have failed in the final steps of clinical trials [49].

In this context, early vaccines against this bacterium targeted the lipopolysaccharide (O-antigen) and could generate satisfactory immunity. However, this protection was LPS serotype-specific, and with more than 30 subtypes of O-antigens, this strategy has met significant challenges [50]. In addition, vaccination with the type III secretion system protein PopB encapsulated into PLGA (polylactic-co-glycolic acid) nanoparticles revealed protection against the lethal *P. aeruginosa* challenge and induced a Th17 response in the mouse model [50]. However, vaccine-induced Th17 responses may be harmful in the situation of cystic fibrosis (CF), because Th17-characterized lung inflammation has been observed in CF patients [51]. Moreover, it was reported that the killed but metabolically active (KBMA) attenuation *P. aeruginosa*-based vaccine induces preventative immunity responses against pulmonary infections [11]. It seems that this type of vaccine has some disadvantages, including the risk of reversion to a virulent strain and safety concerns for immunocompromised people [52]. In addition, the high amount of LPS and its toxicity are other points that should be considered [53].

So far, different *in silico* studies have been conducted to introduce immunogenic targets against this bacterium. For example, Beg *et al.* designed multi-epitope-based vaccines against functional amyloids of *P. aeruginosa* (Fap) using different immunoinformatic and structural bioinformatic approaches [54]. In addition, the computational study conducted by Dey *et al.* mainly focused on *P. aeruginosa's* major membrane proteins, including OprF and OprI, to design peptide-based vaccine constructs [55]. In addition, Elhag and colleagues predicted an epitope-based vaccine against this bacterium using fructose bisphosphate aldolase (FBA) protein through immunoinformatics tools [56]. Although the results of these studies were valuable in finding a promising vaccine against this bacterium, their major limitation was their focus on just one or two bacterial proteins. Meanwhile, the study by Solanki *et al.* was more comprehensive, as they used a comparative subtractive proteomic analysis among 1,191 *P. aeruginosa*

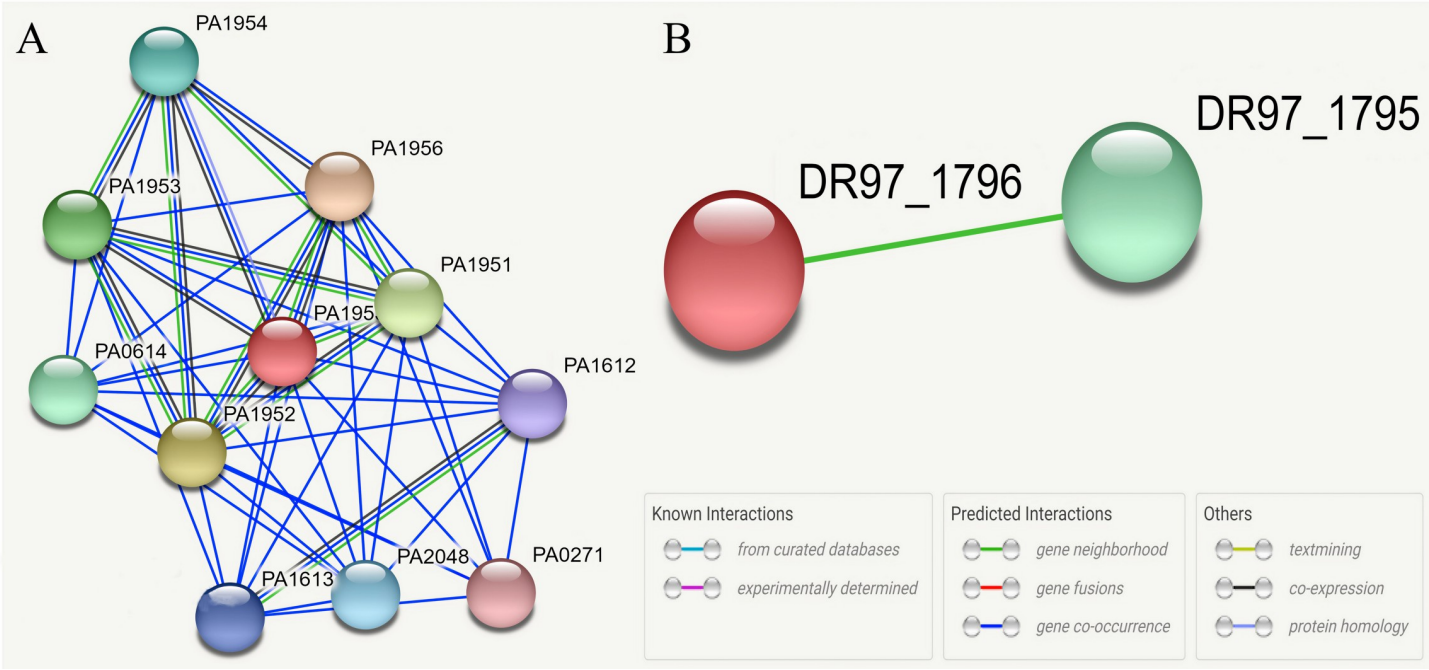

Fig 5. Protein-protein STRING interaction networks of two Hypothetical proteins (e.g. WP_132548232.1 and WP_166796845.1) with other proteins of P. aeruginosa strain 24Pae112. According to obtained result, WP_132548232.1 has co-occurrence and co-expression with Peptidase C39 domain-containing protein (PA1953) and co-occurrence with ABM domain-containing protein (PA0271).

https://doi.org/10.1371/journal.pone.0289609.g005

proteomes and finally left a total of twenty unique and non-redundant proteomes. However, they presented a chimeric vaccine with PADRE (pan-HLA-DR epitopes) as an adjuvant [57] which is completely different from our presented platforms.

In this comprehensive study, it was considered the total proteins of *P. aeruginosa* 24Pae112 and evaluated them from all aspects of immunoinformatics to find novel and putative immunogenic targets. In this regard, different bioinformatics tools and algorithms were used to justify the obtained results. In the case of antigenicity and allergenicity, for example, we used Vaxigen/ANTIGENpro and AlgPred/AllergenFP, respectively. However, we considered only one of them in the study since VaxiJen is the first server for alignment-independent prediction of protective antigens and has been used for antigenicity prediction in many articles on reverse vaccinology [58–60]. In the case of allergenicity, it was found that the results from both databases largely overlapped (only in seven cases were the results different) and we considered the results obtained from AlgPred. Moreover, in the present study, the quartile ranking method was used to select the shortlisted proteins. It should be mentioned that quartile analysis can be a valuable global approach in reverse vaccinology because when selecting the best targets, different criteria such as antigenicity, allergenicity, *etc*. can be taken into account at the same time [61].

The authors of this article believe that using multiple tools for analysis will not always yield the desired results. For example, in subcellular localization, the simultaneous use of several tools to determine the location of proteins in bacteria will be confusing due to different prediction algorithms. Furthermore, we attempted to choose experimental-based tools. However, the accuracy rate of computational tools can be considered as a limitation.

The results of this study are significant, as all 16 shortlisted proteins can be obtained as subunit vaccines for further studies in animal models. These proteins are surface-exposed, have a

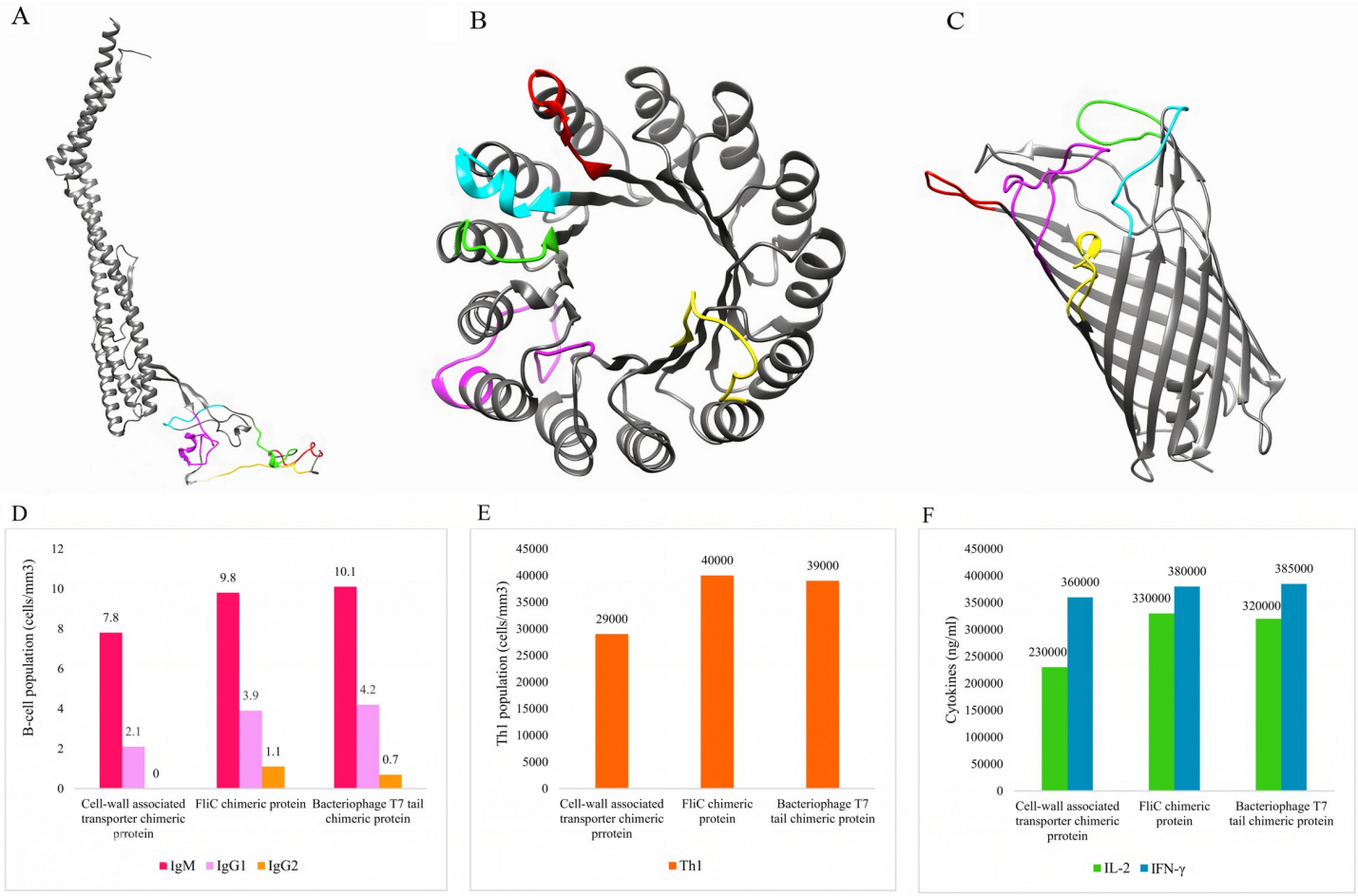

Fig 6. The 3D structures of the multi-epitope vaccines were predicted using the Robetta web tool and validated by the ProSA web server. The linear B-cell epitopes are colored using Jmol software (A-C). In addition, immune simulation of designed vaccines has shown in the Figure (D-E). **A)** The structure and epitopes of chimeric FliC protein, **B)** The bacteriophage T7 tail, and **C)** The cell wall-associated chimeric proteins. **D)** Bacteriophage T7 tail chimeric protein and FliC chimeric protein induced higher levels of IgM, IgG1, and IgG2. **E)** FliC chimeric protein and bacteriophage T7 tail chimeric protein showed higher levels of Th1 cell population production. **F)** A higher level of IL-2 and IFN-γ was induced by the bacteriophage T7 tail and FliC chimeric proteins.

https://doi.org/10.1371/journal.pone.0289609.g006

molecular weight of < 110 kDa, and are capable of inducing both humoral and cellular immunity.

The first group of shortlisted putative vaccine candidates belong to secretion systems and transports, including (I) Type II secretion system secretin GspD (WP_061193930.1), (II) Hcp family type VI secretion system effector (WP_110726056.1), (III) Type III secretion system needle length determinant (WP_210733189.1), and (IV) Transporter (WP_024947839.1). The transport of proteins from the cytoplasm to other parts of the cell or the environment, a process known as secretion, is one of the most important prokaryotic cell functions. Prokaryotes have evolved numerous ways to transport protein cargo between locations, most of which involve the assistance of specialized protein secretion systems. Proteins taking part in secretion systems are essential for bacterial growth and are involved in several processes [62]. Proteins from this group have already been introduced as vaccine candidates against this bacterium. For example, it was reported that immunization of mice with surface-expressed PcrV, the needle-tip protein component of T3SS, resulted in a reduction in cytotoxicity and inflammation and enabled neutrophil internalization of *P. aeruginosa* [63, 64]. Therefore, it can be concluded

Table 2. The thermodynamic interactions of three proposed multi-epitope-based vaccines against *P. aeruginosa* with TLR1, 2, and 4.

Interactions of multi-epitope-based vaccines and TLRs	Total (kcal/mol)	VdW (kcal/mol)	Desolvation (kcal/mol)	Electrostatics (kcal/mol)
FliC -TLR1	-29.006	11.341	-4.547	-25.593
FliC -TLR2	-31.891	30.684	1.918	-36.878
FliC -TLR4	-35.018	23.241	-17.548	-19.794
Bacteriophage T7 tail protein-TLR1	-26.392	-6.142	-0.330	-25.447
Bacteriophage T7 tail protein-TLR2	-23.688	0.488	-11.324	-12.413
Bacteriophage T7 tail protein-TLR4	-32.649	30.339	-21.364	-14.320
Cell-wall associated transporter-TLR1	-67.516	17.263	-46.745	-22.497
Cell-wall associated transporter-TLR2	-52.280	12.465	-40.360	-13.166
Cell-wall associated transporter-TLR4	-69.791	138.816	-69.328	-14.344

*VdW: Van-der-Waals

https://doi.org/10.1371/journal.pone.0289609.t002

that secretion system-associated proteins can play an important role in immunogenicity in addition to pathogenicity in this bacterium.

In the second group, four proteins, including WP_003090815, WP_217385706.1, WP_243702750.1, and WP_019681707.1, belong to the OprD family of outer membrane proteins. This family was identified for the first time during outer membrane investigations of carbapenem-resistant *Acinetobacter baumannii* isolates [65]. The OprD is an orthologous protein and the prototype of a specific channel superfamily notable for its 19 members in *P. aeruginosa*. These proteins demonstrated 46 to 57% similarity and play an important role in amino acid or organic acid uptake. The OprD has been extensively studied based on its structure, function, and involvement in the carbapenem resistance of *P. aeruginosa*. This protein, with an 18-strand barrel structure, forms a very narrow channel with two structural features that may contribute to its channel specificity [66, 67].

In the third group, we introduced fimbrial proteins including, (I) Type I fimbrial protein (WP_034004502.1) and (II) Type IVa pilus secretin PilQ (WP_132905315.1) as a putative vaccine candidate against *P. aeruginosa*. This protein group was previously introduced as vaccine candidates against other Gram-negative bacteria such as *Escherichia coli* [68], *Klebsiella pneumoniae* [69], and *Salmonella enterica* serovar Typhi [69]. Moreover, a study conducted by Gholami *et al*. reported the potential of integrated PilQ/PilA (QA) antigens as a promising vaccine candidate against *P. aeruginosa*. Those study revealed that the chimeric protein PilQ and the disulfide-turn region of PilA trigger the production of specific antibodies in the BALB/c mouse model [70].

In the fourth group, TonB-dependent receptors (WP_023101627.1 and WP_125941151.1) were presented as putative vaccine candidates against *P. aeruginosa*. TonB-dependent receptors are a family of beta-barrel proteins named for their localization in the outer membrane of Gram-negative bacteria. These complexes recognize various signals from outside of the bacterial cells and transduce them into the cytoplasm, resulting in transcriptional activation of target genes [71]. This well-known protein has been previously introduced as a putative vaccine candidate against several Gram-negative bacteria, such as *A. baumannii* [72], *N. gonorrhoeae* [73], and *K. pneumoniae* [74].

In the fifth group, peptidoglycan-associated proteins, including (I) Peptidoglycan-associated lipoprotein Pal (WP_058148283.1) and (II) Glycosyl hydrolase family 18 protein (WP_034004678.1), are among the shortlisted immunogenic targets against *P. aeruginosa*. In Gram-negative bacteria, Pal is related to the integrity of the cellular envelope and interacts powerfully with the peptidoglycan layer [75]. Consistent with our results, it was recently

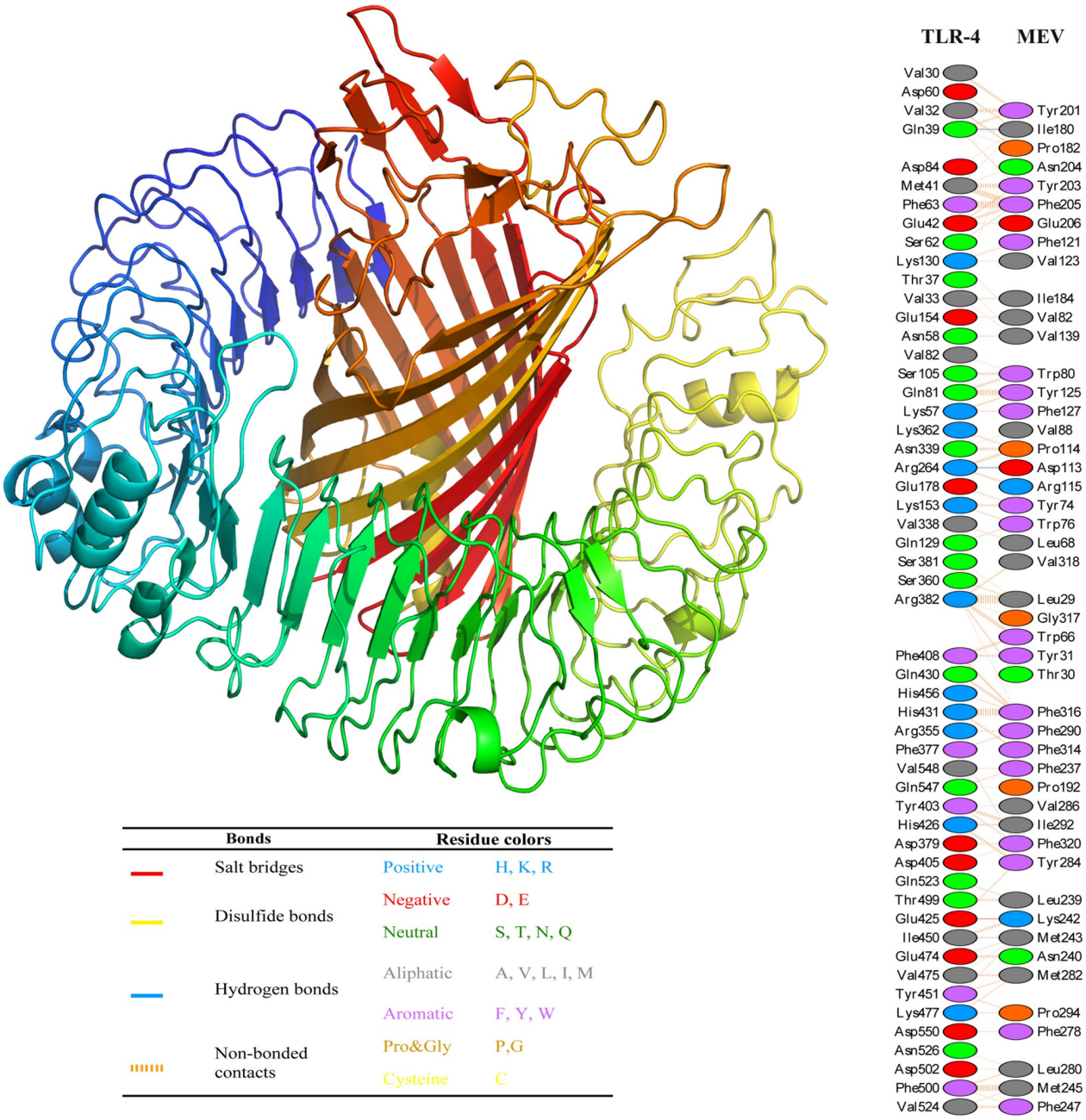

Fig 7. Details of interactions between the chimeric cell-wall-associated transporter and TLR4. The 3D structure prediction of the chimeric cell-wall-associated transporter-TLR4 complex was illustrated using the UCSF Chimera software. The paired residue's interactions between cell-wall-associated transporter and TLR4 have shown with different colors (Table is near here.) in the Figure.

https://doi.org/10.1371/journal.pone.0289609.g007

reported that the peptidoglycan-associated lipoprotein Pal is a critical virulence determinant of *Burkholderia mallei* and could be considered an effective target for developing a vaccine against glander [76].

Finally, the Hypothetical protein WP_132548232.1 has co-occurrence and co-expression with peptidase C39 domain-containing proteins and co-occurrence with ABM domain-containing proteins. The peptidase C39 domain-containing protein defined by this cysteine

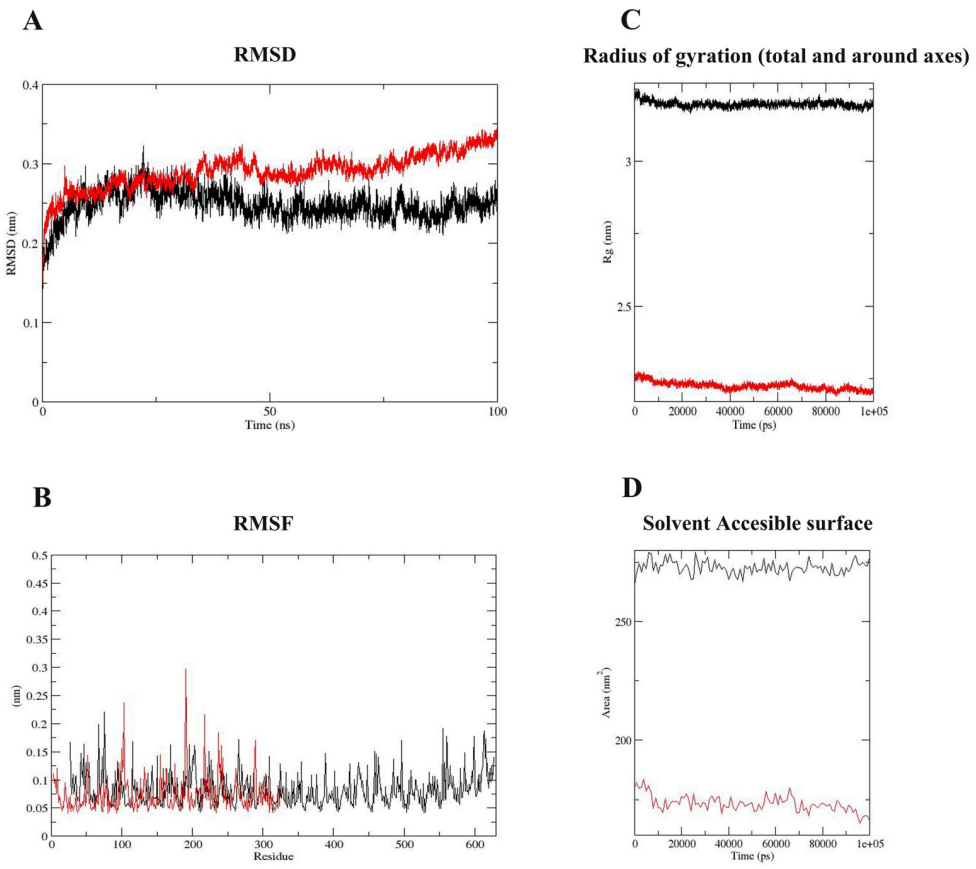

Fig 8. Molecular dynamics (MD) simulation results. A) According to the RMSD plot, TLR4 and cell-wall- associated transporter were in the range of 0.2 to 0.27 and 0.2 to 0.3, respectively. This result indicates that both proteins reach stability at time 10 and remain physically stable after that. **B)** The obtained result from the RMSF plot demonstrated that no unusual fluctuation was observed in protein structures. **C)** According to the Rg result, the structures of cell-wall-associated transporter and TLR4 were stable. **D)** The SASA of cell-wall-associated transporter and TLR4 was in the range of 168 to 18 nm^2 and 270 to 277 nm^2, respectively. In all Figures, TLR4 and complex (including TLR4 and chimeric cell-wall-associated transporter) are presented in red and block colors, respectively.

https://doi.org/10.1371/journal.pone.0289609.g008

peptidase domain belongs to the peptidase family C39 (clan CA). It is found in a wide range of ABC transporters, which are maturation proteases for peptide bacteriocins, with the proteolytic domain located in the N-terminal region of the protein [77]. On the other hand, the Hypothetical protein WP_166796845.1 is neighboring the UvrD/REP helicase N-terminal domain protein. UvrD helicase is a multi-domain DNA helicase that has a molecular weight of 82 kDa [78].

A multi-epitope vaccine composed of a series of peptides is an ideal approach for the prevention and treatment of bacterial or viral infections [79]. Introducing cell-wall-associated transporter and bacteriophage T7 tail chimeric proteins as multi-epitope vaccines against *P. aeruginosa* and suitable scaffolds for multi-epitope vaccine design and development was the significant novelty of the present study. These new platforms for vaccine design can be used not only against *P. aeruginosa* but also against other bacteria. The disordered regions of these proteins are proper for the implantation of conserved and antigenic epitopes from different pathogens to induce a satisfactory immune response. Cell-wall-associated transporter had the strongest interactions with TLR 1, 2, and 4. TLRs are the major mediators of inflammatory pathways, playing important roles in mediating immune responses to a variety of pathogen-derived ligands and linking adaptive immunity to innate immunity [80]. On the other hand,

the bacteriophage T7 tail chimeric protein had the strongest ability to stimulate the immune response. This result showed the better performance of these two platforms compared to the FliC, which is a known platform for multi-epitope vaccine design [81].

5. Conclusion

This comprehensive study evaluated the entire genome sequence of *P. aeruginosa* strain 24Pae112 to find novel and putative immunogenic targets. The results of this study are significant, as all 16 proteins presented are valuable for further investigation in animal models. These proteins were classified into six different groups according to their conserved domains, including (I) Secretion system-associated proteins and transporters, (II) OprD family outer membrane proteins, (III) Fimbrial proteins, (IV) TonB dependent receptors, (V) Peptidoglycan-associated proteins, and (VI) Unknown-function proteins (Hypothetical proteins). On the other hand, three designed multi-epitope vaccines showed promising results. Finally, it is worth noting that two proteins (*e.g.* cell-wall-associated transporter and bacteriophage T7 tail chimeric protein) as new platforms for vaccine design and development can be used not only against *P. aeruginosa* but also against other superbugs. We hope these two platforms will receive more investigation in future studies.

Supporting information

S1 Fig. Quality assessment of tertiary structures of 16 shortlisted proteins using ProSA web server and Ramachandran plots.
(PDF)

S1 Table. The molecular weight, functional class, conserved domain, and prevalence prediction of 72 selected proteins against *P. aeruginosa* 24Pae112.
(DOCX)

S2 Table. Evaluation of linear B-cell epitopes and design of different multi-epitope vaccines against *P. aeruginosa* 24Pae112.
(DOCX)

Acknowledgments

The authors of this article will thank the personnel at the Pasteur Institute of Iran for their support.

Author Contributions

Conceptualization: Farzad Badmasti.

Data curation: Sepideh Fereshteh.

Investigation: Narjes Noori Goodarzi, Behnoush Khasheii, Farzad Badmasti.

Methodology: Sepideh Fereshteh, Narjes Noori Goodarzi, Mahdi Torkamaneh, Behnoush Khasheii.

Software: Fatemeh Haririzadeh Jouriani, Mahdi Torkamaneh.

Validation: Sepideh Fereshteh, Fatemeh Haririzadeh Jouriani.

Visualization: Sepideh Fereshteh, Fatemeh Haririzadeh Jouriani, Narjes Noori Goodarzi, Mahdi Torkamaneh.

Writing – original draft: Sepideh Fereshteh, Fatemeh Haririzadeh Jouriani.

Writing – review & editing: Farzad Badmasti.

References

1. Pang Z, Raudonis R, Glick BR, Lin T-J, Cheng Z. Antibiotic resistance in Pseudomonas aeruginosa: mechanisms and alternative therapeutic strategies. Biotechnology advances. 2019; 37(1):177–92. https://doi.org/10.1016/j.biotechadv.2018.11.013 PMID: 30500353
2. Thi MTT, Wibowo D, Rehm BH. Pseudomonas aeruginosa biofilms. International journal of molecular sciences. 2020; 21(22):8671. https://doi.org/10.3390/ijms21228671 PMID: 33212950
3. Gomila A, Carratalà J, Badia JM, Camprubí D, Piriz M, Shaw E, et al. Preoperative oral antibiotic prophylaxis reduces Pseudomonas aeruginosa surgical site infections after elective colorectal surgery: a multicenter prospective cohort study. BMC Infectious Diseases. 2018; 18(1):1–9.
4. Murphy TF. Pseudomonas aeruginosa in adults with chronic obstructive pulmonary disease. Current opinion in pulmonary medicine. 2009; 15(2):138–42. https://doi.org/10.1097/MCP.0b013e328321861a PMID: 19532029
5. Organization WH. Prioritization of pathogens to guide discovery, research and development of new antibiotics for drug-resistant bacterial infections, including tuberculosis. World Health Organization, 2017 9240026436.
6. Hirsch EB, Tam VH. Impact of multidrug-resistant Pseudomonas aeruginosa infection on patient outcomes. Expert review of pharmacoeconomics & outcomes research. 2010; 10(4):441–51. https://doi.org/10.1586/erp.10.49 PMID: 20715920
7. Solanki V, Tiwari M, Tiwari V. Prioritization of potential vaccine targets using comparative proteomics and designing of the chimeric multi-epitope vaccine against Pseudomonas aeruginosa. Scientific reports. 2019; 9(1):1–19.
8. Wan C, Zhang J, Zhao L, Cheng X, Gao C, Wang Y, et al. Rational design of a chimeric derivative of PcrV as a subunit vaccine against Pseudomonas aeruginosa. Frontiers in immunology. 2019; 10:781. https://doi.org/10.3389/fimmu.2019.00781 PMID: 31068928
9. Cripps AW, Peek K, Dunkley M, Vento K, Marjason JK, McIntyre ME, et al. Safety and immunogenicity of an oral inactivated whole-cell Pseudomonas aeruginosa vaccine administered to healthy human subjects. Infection and immunity. 2006; 74(2):968–74. https://doi.org/10.1128/IAI.74.2.968-974.2006 PMID: 16428742
10. Kamei A, Coutinho-Sledge YS, Goldberg JB, Priebe GP, Pier GB. Mucosal vaccination with a multivalent, live-attenuated vaccine induces multifactorial immunity against Pseudomonas aeruginosa acute lung infection. Infection and immunity. 2011; 79(3):1289–99. https://doi.org/10.1128/IAI.01139-10 PMID: 21149583
11. Meynet E, Laurin D, Lenormand JL, Camara B, Toussaint B, Le Gouëllec A. Killed but metabolically active Pseudomonas aeruginosa-based vaccine induces protective humoral-and cell-mediated immunity against Pseudomonas aeruginosa pulmonary infections. Vaccine. 2018; 36(14):1893–900. https://doi.org/10.1016/j.vaccine.2018.02.040 PMID: 29506924
12. Zhang X, Yang F, Zou J, Wu W, Jing H, Gou Q, et al. Immunization with Pseudomonas aeruginosa outer membrane vesicles stimulates protective immunity in mice. Vaccine. 2018; 36(8):1047–54. https://doi.org/10.1016/j.vaccine.2018.01.034 PMID: 29406241
13. Chirani AS, Majidzadeh R, Pouriran R, Heidary M, Nasiri MJ, Gholami M, et al. The effect of in silico targeting Pseudomonas aeruginosa patatin-like protein D, for immunogenic administration. Computational biology and chemistry. 2018; 74:12–9. https://doi.org/10.1016/j.compbiolchem.2018.02.001 PMID: 29524839
14. Saha S, Takeshita F, Matsuda T, Jounai N, Kobiyama K, Matsumoto T, et al. Blocking of the TLR5 activation domain hampers protective potential of flagellin DNA vaccine. The Journal of Immunology. 2007; 179(2):1147–54. https://doi.org/10.4049/jimmunol.179.2.1147 PMID: 17617608
15. Micoli F, Costantino P, Adamo R. Potential targets for next generation antimicrobial glycoconjugate vaccines. FEMS microbiology reviews. 2018; 42(3):388–423. https://doi.org/10.1093/femsre/fuy011 PMID: 29547971
16. Grandi G. Bacterial surface proteins and vaccines. F1000 biology reports. 2010; 2. https://doi.org/10.3410/B2-36 PMID: 20948798
17. Sette A, Rappuoli R. Reverse vaccinology: developing vaccines in the era of genomics. Immunity. 2010; 33(4):530–41. https://doi.org/10.1016/j.immuni.2010.09.017 PMID: 21029963
18. Bahadori Z, Shafaghi M, Madanchi H, Ranjbar MM, Shabani AA, Mousavi SF. In silico designing of a novel epitope-based candidate vaccine against Streptococcus pneumoniae with introduction of a new domain of PepO as adjuvant. Journal of translational medicine. 2022; 20(1):1–28.

19. Medini D, Stella M, Wassil J. MATS: Global coverage estimates for 4CMenB, a novel multicomponent meningococcal B vaccine. Vaccine. 2015; 33(23):2629–36. https://doi.org/10.1016/j.vaccine.2015.04.015 PMID: 25882169

20. Serruto D, Bottomley MJ, Ram S, Giuliani MM, Rappuoli R. The new multicomponent vaccine against meningococcal serogroup B, 4CMenB: immunological, functional and structural characterization of the antigens. Vaccine. 2012; 30:B87–B97. https://doi.org/10.1016/j.vaccine.2012.01.033 PMID: 22607904

21. Nasiri O, Hajihassani M, Noori Goodarzi N, Fereshteh S, Bolourchi N, Firoozeh F, et al. Reverse vaccinology approach to identify novel and immunogenic targets against Porphyromonas gingivalis: An in silico study. Plos one. 2022; 17(8):e0273770. https://doi.org/10.1371/journal.pone.0273770 PMID: 36040920

22. Chaudhari NM, Gupta VK, Dutta C. BPGA-an ultra-fast pan-genome analysis pipeline. Scientific reports. 2016; 6(1):1–10.

23. Treepong P, Kos V, Guyeux C, Blanc D, Bertrand X, Valot B, et al. Global emergence of the widespread Pseudomonas aeruginosa ST235 clone. Clinical Microbiology and Infection. 2018; 24(3):258–66. https://doi.org/10.1016/j.cmi.2017.06.018 PMID: 28648860

24. Gardy JL, Laird MR, Chen F, Rey S, Walsh C, Ester M, et al. PSORTb v. 2.0: expanded prediction of bacterial protein subcellular localization and insights gained from comparative proteome analysis. Bioinformatics. 2005; 21(5):617–23. https://doi.org/10.1093/bioinformatics/bti057 PMID: 15501914

25. Käll L, Krogh A, Sonnhammer EL. Advantages of combined transmembrane topology and signal peptide prediction—the Phobius web server. Nucleic acids research. 2007; 35(suppl_2):W429–W32. https://doi.org/10.1093/nar/gkm256 PMID: 17483518

26. Doytchinova IA, Flower DR. VaxiJen: a server for prediction of protective antigens, tumour antigens and subunit vaccines. BMC bioinformatics. 2007; 8(1):1–7. https://doi.org/10.1186/1471-2105-8-4 PMID: 17207271

27. Magnan CN, Zeller M, Kayala MA, Vigil A, Randall A, Felgner PL, et al. High-throughput prediction of protein antigenicity using protein microarray data. Bioinformatics. 2010; 26(23):2936–43. https://doi.org/10.1093/bioinformatics/btq551 PMID: 20934990

28. Sharma N, Patiyal S, Dhall A, Pande A, Arora C, Raghava GP. AlgPred 2.0: an improved method for predicting allergenic proteins and mapping of IgE epitopes. Briefings in Bioinformatics. 2021; 22(4): bbaa294. https://doi.org/10.1093/bib/bbaa294 PMID: 33201237

29. Dimitrov I, Naneva L, Doytchinova I, Bangov I. AllergenFP: allergenicity prediction by descriptor fingerprints. Bioinformatics. 2014; 30(6):846–51. https://doi.org/10.1093/bioinformatics/btt619 PMID: 24167156

30. Mahram A, Herbordt MC. NCBI BLASTP on high-performance reconfigurable computing systems. ACM Transactions on Reconfigurable Technology and Systems (TRETS). 2015; 7(4):1–20.

31. Saha S, Raghava G. VICMpred: an SVM-based method for the prediction of functional proteins of Gram-negative bacteria using amino acid patterns and composition. Genomics, proteomics & bioinformatics. 2006; 4(1):42–7. https://doi.org/10.1016/S1672-0229(06)60015-6 PMID: 16689701

32. Roy S, Maheshwari N, Chauhan R, Sen NK, Sharma A. Structure prediction and functional characterization of secondary metabolite proteins of Ocimum. Bioinformation. 2011; 6(8):315–9. https://doi.org/10.6026/97320630006315 PMID: 21769194

33. Marchler-Bauer A, Anderson JB, Cherukuri PF, DeWeese-Scott C, Geer LY, Gwadz M, et al. CDD: a Conserved Domain Database for protein classification. Nucleic acids research. 2005; 33(suppl_1): D192–D6. https://doi.org/10.1093/nar/gki069 PMID: 15608175

34. Huerta-Cepas J, Szklarczyk D, Forslund K, Cook H, Heller D, Walter MC, et al. eggNOG 4.5: a hierarchical orthology framework with improved functional annotations for eukaryotic, prokaryotic and viral sequences. Nucleic acids research. 2016; 44(D1):D286–D93. https://doi.org/10.1093/nar/gkv1248 PMID: 26582926

35. Pourseif MM, Moghaddam G, Naghili B, Saeedi N, Parvizpour S, Nematollahi A, et al. A novel in silico minigene vaccine based on CD4+ T-helper and B-cell epitopes of EG95 isolates for vaccination against cystic echinococcosis. Computational Biology and Chemistry. 2018; 72:150–63. https://doi.org/10.1016/j.compbiolchem.2017.11.008 PMID: 29195784

36. Paul S, Sidney J, Sette A, Peters B. TepiTool: a pipeline for computational prediction of T cell epitope candidates. Current protocols in immunology. 2016; 114(1):18.9. 1–.9. 24. https://doi.org/10.1002/cpim.12 PMID: 27479659

37. Kim DE, Chivian D, Baker D. Protein structure prediction and analysis using the Robetta server. Nucleic acids research. 2004; 32(suppl_2):W526–W31. https://doi.org/10.1093/nar/gkh468 PMID: 15215442

38. Wiederstein M, Sippl MJ. ProSA-web: interactive web service for the recognition of errors in three-dimensional structures of proteins. Nucleic acids research. 2007; 35(suppl_2):W407–W10. https://doi.org/10.1093/nar/gkm290 PMID: 17517781

39. Anderson RJ, Weng Z, Campbell RK, Jiang X. Main-chain conformational tendencies of amino acids. Proteins: Structure, Function, and Bioinformatics. 2005; 60(4):679–89.

40. Ponomarenko J, Bui H-H, Li W, Fusseder N, Bourne PE, Sette A, et al. ElliPro: a new structure-based tool for the prediction of antibody epitopes. BMC bioinformatics. 2008; 9(1):1–8. https://doi.org/10.1186/1471-2105-9-514 PMID: 19055730

41. Herraez A. Biomolecules in the computer: Jmol to the rescue. Biochemistry and Molecular Biology Education. 2006; 34(4):255–61. https://doi.org/10.1002/bmb.2006.494034042644 PMID: 21638687

42. Szklarczyk D, Kirsch R, Koutrouli M, Nastou K, Mehryary F, Hachilif R, et al. The STRING database in 2023: protein–protein association networks and functional enrichment analyses for any sequenced genome of interest. Nucleic acids research. 2023; 51(D1):D638–D46. https://doi.org/10.1093/nar/gkac1000 PMID: 36370105

43. Glaser F, Pupko T, Paz I, Bell RE, Bechor-Shental D, Martz E, et al. ConSurf: identification of functional regions in proteins by surface-mapping of phylogenetic information. Bioinformatics. 2003; 19(1):163–4. https://doi.org/10.1093/bioinformatics/19.1.163 PMID: 12499312

44. Laskowski RA. PDBsum: summaries and analyses of PDB structures. Nucleic acids research. 2001; 29 (1):221–2. https://doi.org/10.1093/nar/29.1.221 PMID: 11125097

45. Bahadori Z, Shafaghi M, Madanchi H, Ranjbar MM, Shabani AA, Mousavi SF. In silico designing of a novel epitope-based candidate vaccine against Streptococcus pneumoniae with introduction of a new domain of PepO as adjuvant. Journal of Translational Medicine. 2022; 20(1):389. https://doi.org/10.1186/s12967-022-03590-6 PMID: 36059030

46. Shafaghi M, Bahadori Z, Madanchi H, Ranjbar MM, Shabani AA, Mousavi SF. Immunoinformatics-aided design of a new multi-epitope vaccine adjuvanted with domain 4 of pneumolysin against Streptococcus pneumoniae strains. BMC bioinformatics. 2023; 24(1):1–27.

47. Bassetti M, Vena A, Croxatto A, Righi E, Guery B. How to manage Pseudomonas aeruginosa infections. Drugs in context. 2018; 7.

48. Pena C, Suarez C, Tubau F, Dominguez A, Sora M, Pujol M, et al. Carbapenem-resistant Pseudomonas aeruginosa: factors influencing multidrug-resistant acquisition in non-critically ill patients. European journal of clinical microbiology & infectious diseases. 2009; 28(5):519–22. https://doi.org/10.1007/s10096-008-0645-9 PMID: 18949495

49. Merakou C, Schaefers MM, Priebe GP. Progress toward the elusive Pseudomonas aeruginosa vaccine. Surgical infections. 2018; 19(8):757–68. https://doi.org/10.1089/sur.2018.233 PMID: 30388058

50. Schaefers MM, Duan B, Mizrahi B, Lu R, Reznor G, Kohane DS, et al. PLGA-encapsulation of the Pseudomonas aeruginosa PopB vaccine antigen improves Th17 responses and confers protection against experimental acute pneumonia. Vaccine. 2018; 36(46):6926–32. https://doi.org/10.1016/j.vaccine.2018.10.010 PMID: 30314911

51. Tan H-L, Regamey N, Brown S, Bush A, Lloyd CM, Davies JC. The Th17 pathway in cystic fibrosis lung disease. American journal of respiratory and critical care medicine. 2011; 184(2):252–8. https://doi.org/10.1164/rccm.201102-0236OC PMID: 21474644

52. Shkap V, de Vos AJ, Zweygarth E, Jongejan F. Attenuated vaccines for tropical theileriosis, babesiosis and heartwater: the continuing necessity. Trends in parasitology. 2007; 23(9):420–6. https://doi.org/10.1016/j.pt.2007.07.003 PMID: 17656155

53. Ciesielska A, Matyjek M, Kwiatkowska K. TLR4 and CD14 trafficking and its influence on LPS-induced pro-inflammatory signaling. Cellular and molecular life sciences. 2021; 78(4):1233–61. https://doi.org/10.1007/s00018-020-03656-y PMID: 33057840

54. Beg AZ, Farhat N, Khan AU. Designing multi-epitope vaccine candidates against functional amyloids in Pseudomonas aeruginosa through immunoinformatic and structural bioinformatics approach. Infection, Genetics and Evolution. 2021; 93:104982. https://doi.org/10.1016/j.meegid.2021.104982 PMID: 34186254

55. Dey J, Mahapatra SR, Patnaik S, Lata S, Kushwaha GS, Panda RK, et al. Molecular Characterization and Designing of a Novel Multiepitope Vaccine Construct Against Pseudomonas aeruginosa. Int J Pept Res Ther. 2022; 28(2):49. Epub 2022/01/25. https://doi.org/10.1007/s10989-021-10356-z PMID: 35069055; PubMed Central PMCID: PMC8762192.

56. Elhag M, Alaagib RM, Ahmed NM, Abubaker M, Haroun EM, Albagi SOA, et al. Design of Epitope-Based Peptide Vaccine against Pseudomonas aeruginosa Fructose Bisphosphate Aldolase Protein Using Immunoinformatics. J Immunol Res. 2020; 2020:9475058. Epub 2020/11/19. https://doi.org/10.1155/2020/9475058 PMID: 33204735; PubMed Central PMCID: PMC7666636.

57. Solanki V, Tiwari M, Tiwari V. Prioritization of potential vaccine targets using comparative proteomics and designing of the chimeric multi-epitope vaccine against Pseudomonas aeruginosa. Sci Rep. 2019; 9(1):5240. Epub 2019/03/29. https://doi.org/10.1038/s41598-019-41496-4 PMID: 30918289; PubMed Central PMCID: PMC6437148.

58. Doytchinova IA, Flower DR. VaxiJen: a server for prediction of protective antigens, tumour antigens and subunit vaccines. BMC Bioinformatics. 2007; 8:4. Epub 2007/01/09. https://doi.org/10.1186/1471-2105-8-4 PMID: 17207271; PubMed Central PMCID: PMC1780059.

59. Bibi S, Ullah I, Zhu B, Adnan M, Liaqat R, Kong WB, et al. In silico analysis of epitope-based vaccine candidate against tuberculosis using reverse vaccinology. Sci Rep. 2021; 11(1):1249. Epub 2021/01/15. https://doi.org/10.1038/s41598-020-80899-6 PMID: 33441913; PubMed Central PMCID: PMC7807040.

60. Jalal K, Abu-Izneid T, Khan K, Abbas M, Hayat A, Bawazeer S, et al. Identification of vaccine and drug targets in Shigella dysenteriae sd197 using reverse vaccinology approach. Sci Rep. 2022; 12(1):251. Epub 2022/01/09. https://doi.org/10.1038/s41598-021-03988-0 PMID: 34997046; PubMed Central PMCID: PMC8742002.

61. Shahbazi S, Sabzi S, Goodarzi NN, Fereshteh S, Bolourchi N, Mirzaie B, et al. Identification of novel putative immunogenic targets and construction of a multi-epitope vaccine against multidrug-resistant Corynebacterium jeikeium using reverse vaccinology approach. Microbial Pathogenesis. 2022; 164:105425. https://doi.org/10.1016/j.micpath.2022.105425 PMID: 35114352

62. Green ER, Mecsas J. Bacterial secretion systems: an overview. Microbiology spectrum. 2016; 4(1):4.1.13. https://doi.org/10.1128/microbiolspec.VMBF-0012-2015 PMID: 26999395

63. Lynch SV, Flanagan JL, Sawa T, Fang A, Baek MS, Rubio-Mills A, et al. Polymorphisms in the Pseudomonas aeruginosa type III secretion protein, PcrV–implications for anti-PcrV immunotherapy. Microbial pathogenesis. 2010; 48(6):197–204. https://doi.org/10.1016/j.micpath.2010.02.008 PMID: 20211240

64. Tian L, Xu S, Hutchins WC, Yang C-H, Li J. Impact of the exopolysaccharides Pel and Psl on the initial adhesion of Pseudomonas aeruginosa to sand. Biofouling. 2014; 30(2):213–22. https://doi.org/10.1080/08927014.2013.857405 PMID: 24404893

65. Dupont M, Pagès J-M, Lafitte D, Siroy A, Bollet C. Identification of an OprD Homologue in Acinetobacter b aumannii. Journal of proteome research. 2005; 4(6):2386–90. https://doi.org/10.1021/pr050143q PMID: 16335991

66. Tamber S, Ochs MM, Hancock RE. Role of the novel OprD family of porins in nutrient uptake in Pseudomonas aeruginosa. Journal of bacteriology. 2006; 188(1):45–54. https://doi.org/10.1128/JB.188.1.45-54.2006 PMID: 16352820

67. Catel-Ferreira M, Nehmé R, Molle V, Aranda J, Bouffartigues E, Chevalier S, et al. Deciphering the function of the outer membrane protein OprD homologue of Acinetobacter baumannii. Antimicrobial agents and chemotherapy. 2012; 56(7):3826–32. https://doi.org/10.1128/AAC.06022-11 PMID: 22564848

68. Liu Y, Maciel Jr M, O'Dowd A, Poole ST, Rollenhagen JE, Etobayeva IV, et al. Development and Comparison of a Panel of Modified CS17 Fimbrial Tip Adhesin Proteins as Components for an Adhesin-Based Vaccine against Enterotoxigenic Escherichia coli. Microorganisms. 2021; 9(8):1646. https://doi.org/10.3390/microorganisms9081646 PMID: 34442726

69. Esmailnia E, Amani J, Gargari SLM. Identification of novel vaccine candidate against Salmonella enterica serovar Typhi by reverse vaccinology method and evaluation of its immunization. Genomics. 2020; 112(5):3374–81. https://doi.org/10.1016/j.ygeno.2020.06.022 PMID: 32565239

70. Gholami M, Chirani A, Razavi S, Falak R, Irajian G. Immunogenicity of a fusion protein containing PilQ and disulphide turn region of PilA from Pseudomonas aeruginosa in mice. Letters in applied microbiology. 2017; 65(5):439–45. https://doi.org/10.1111/lam.12796 PMID: 28857243

71. Koebnik R, Locher KP, Van Gelder P. Structure and function of bacterial outer membrane proteins: barrels in a nutshell. Molecular microbiology. 2000; 37(2):239–53. https://doi.org/10.1046/j.1365-2958.2000.01983.x PMID: 10931321

72. Abdollahi S, Rasooli I, Gargari SLM. An in silico structural and physicochemical characterization of TonB-dependent copper receptor in A. baumannii. Microbial pathogenesis. 2018; 118:18–31. https://doi.org/10.1016/j.micpath.2018.03.009 PMID: 29524546

73. Cornelissen CN, Hollander A. TonB-dependent transporters expressed by Neisseria gonorrhoeae. Frontiers in microbiology. 2011; 2:117. https://doi.org/10.3389/fmicb.2011.00117 PMID: 21747812

74. Hsieh P-F, Lin T-L, Lee C-Z, Tsai S-F, Wang J-T. Serum-induced iron-acquisition systems and TonB contribute to virulence in Klebsiella pneumoniae causing primary pyogenic liver abscess. Journal of Infectious Diseases. 2008; 197(12):1717–27. https://doi.org/10.1086/588383 PMID: 18433330

75. Santos CA, Souza AP. Solubilization, Folding, and Purification of a Recombinant Peptidoglycan-Associated Lipoprotein (PAL) Expressed in Escherichia coli. Current Protocols in Protein Science. 2018; 92 (1):e53. https://doi.org/10.1002/cpps.53 PMID: 30040210

76. Dyke JS, Huertas-Diaz MC, Michel F, Holladay NE, Hogan RJ, He B, et al. The Peptidoglycan-associated lipoprotein Pal contributes to the virulence of Burkholderia mallei and provides protection against lethal aerosol challenge. Virulence. 2020; 11(1):1024–40. https://doi.org/10.1080/21505594.2020.1804275 PMID: 32799724

77. Rawlings ND, Barrett AJ. [13] Evolutionary families of metallopeptidases. Methods in enzymology. 248: Elsevier; 1995. p. 183–228.

78. Kawale AA, Burmann BM. UvrD helicase–RNA polymerase interactions are governed by UvrD's carboxy-terminal Tudor domain. Communications biology. 2020; 3(1):607. https://doi.org/10.1038/s42003-020-01332-2 PMID: 33097771

79. Chauhan V, Rungta T, Goyal K, Singh MP. Designing a multi-epitope based vaccine to combat Kaposi Sarcoma utilizing immunoinformatics approach. Scientific reports. 2019; 9(1):1–15.

80. Sameer AS, Nissar S. Toll-like receptors (TLRs): Structure, functions, signaling, and role of their polymorphisms in colorectal cancer susceptibility. BioMed Research International. 2021; 2021. https://doi.org/10.1155/2021/1157023 PMID: 34552981

81. Abadi MHJN, Abyaneh FA, Zare N, Zamani J, Abdoli A, Aslanbeigi F, et al. In silico design and immunoinformatics analysis of a chimeric vaccine construct based on Salmonella pathogenesis factors. Microbial Pathogenesis. 2023; 180:106130. https://doi.org/10.1016/j.micpath.2023.106130 PMID: 37121524